

# AN IMPROVED LIGHTHILL'S ANALYSIS OF HEAT TRANSFER THROUGH BOUNDARY LAYERS

B. T. CHAO

University of Illinois at Urbana-Champaign, Urbana, Illinois, U.S.A.

(Received 13 August 1971)

**Abstract**—Lighthill's investigation of heat transfer through laminar boundary layers has been improved by incorporating the effect of the streamwise pressure gradient on the velocity field. The analysis employs a unique coordinate transformation which makes it possible to express the solution of the governing energy boundary layer equation in terms of a sequence of universal functions. For fluids with Prandtl number of the order unity or larger, only a limited number of these functions are needed. They have been evaluated and tabulated.

To demonstrate the extent of improvement over the analysis of Lighthill, two specific cases are considered. The first is the determination of heat transfer in boundary layers over wedges with a step change in surface temperature. The second is concerned with the evaluation of local Nusselt number over the front portion of a circular cylinder of uniform surface temperature in cross flow. Significant improvement is achieved in both cases.

## NOMENCLATURE

$c_p$ ,	specific heat at constant pressure;
$dp/dx$ ,	streamwise pressure gradient;
$k$ ,	thermal conductivity;
$Pr$ ,	Prandtl number;
$q$ ,	heat flux;
$T$ ,	temperature;
$u$ ,	velocity component in $x$ -direction;
$v$ ,	velocity component in $y$ -direction;
$x$ ,	coordinate measured along the surface and in streamwise direction;
$y$ ,	coordinate normal to the surface;
$z$ ,	Howarth variable, defined in (9);
$\Gamma(n, x)$ ,	incomplete gamma function
	$\int_0^x t^{n-1} e^{-t} dt$ ;
$\varepsilon$ ,	pressure gradient to wall shear parameter, defined in (25);
$\theta$ ,	dimensionless temperature, defined in (7) for compressible flow and in (18) for incompressible flow;
$\mu$ ,	dynamic viscosity;
$\xi$ ,	dimensionless coordinate, defined in (21b, c) for compressible flow and in (22) for incompressible flow;

$\rho$ ,	mass density;
$\tau_w$ ,	shear stress at wall.

## Subscripts

$aw$ ,	refers to adiabatic wall condition;
$e$ ,	refers to outer edge of boundary layer;
$w$ ,	refers to wall condition;
$\infty$ ,	refers to free stream condition.

Other symbols are defined in the text.

## 1. INTRODUCTION

LIGHTHILL's [1] analysis of heat transfer through laminar boundary layers with arbitrary distributions of free-stream velocity and body surface temperature has been the cornerstone of many subsequent investigations. Following the work of Fage and Falkner, Lighthill assumed a linear velocity distribution, i.e.

$$u = \frac{\tau_w(x)}{\mu} y, \quad (1)$$

transformed the energy boundary layer equation into the von Mises form and obtained the solution by the Heaviside operational technique. His equation for the wall heat transfer rate is an approximation for large Prandtl number and is asymptotically exact as  $Pr$  tends to infinity. Based on the integral form of the energy equation and an assumption of similarity between the velocity and the enthalpy profiles, Liepmann [2] presented a simple derivation of Lighthill's formula, generalized for compressible flow. Liepmann also modified the analysis for flow near separation, for which he wrote

$$u = \frac{1}{2\mu_w} \frac{dp}{dx} y^2. \quad (2)$$

To extend the applicability of Lighthill's result, the effect of streamwise pressure gradient on the velocity field must be properly accounted for. This consideration led Spalding [3] to adopt the following expression for the velocity distribution.

$$u = \left( \frac{\partial u}{\partial y} \right)_w y + \frac{1}{2} \left( \frac{\partial^2 u}{\partial y^2} \right)_w y^2 = \frac{\tau_w}{\mu} y + \frac{1}{2\mu} \frac{dp}{dx} y^2 \quad (3)$$

which is a combination of the linear and quadratic distribution prescribed by (1) and (2). For incompressible flows,  $(\partial^3 u / \partial y^3)_w = 0$  and (3) represents, in effect, three terms in the Taylor expansion. Spalding pointed out that the correction to Lighthill's analysis would depend on the relative importance of the second term on the righthand side of (3). The ratio of the second term to the first is

$$\frac{1}{2\tau_w} \frac{dp}{dx} y$$

in which Spalding replaced the variable  $y$  by  $-k(T_w - T_\infty)/q_w$ . As we shall soon see, a different and, perhaps, physically more meaningful length scale arises naturally in the present analysis. Spalding's method was based on the integral energy equation and its use involves iteration. An excellent account of the several attempts to improve Lighthill's result is given in Curle's book [4].

Recently Spence and Brown [5] re-examined the problem and sought solutions of the differential equation for the energy boundary layer. They followed a procedure similar to that used by Lighthill but retained both the linear and quadratic terms in the velocity profile. In order to accommodate compressibility, the  $y$ -coordinate is replaced by the Howarth variable. Heat was considered to diffuse as a passive scalar, without affecting the velocity and density distributions in the layer. These authors were mainly concerned with heat transfer from a *small* surface element maintained at a constant temperature above that of the surrounding adiabatic wall, as this represents the operation of sensors employed by Bellhouse and Schulz [6] and by Brown [7] for the experimental determination of skin friction. Spence and Brown deleted a complicated term in the governing energy equation which vanishes when  $\tau_w^3/(dp/dx)^2$  is constant. While such simplification is valid for the analysis of the performance characteristics of the thin-film skin friction sensor, it cannot be justified in general. They described the original energy boundary layer equation without the said simplification as 'intractable'.

In this paper, an altogether different solution procedure is pursued. The compressible energy boundary layer equation is solved under the usual restrictions. The solution is expressed in terms of universal functions which can be tabulated once and for all. By assigning all fluid properties as constants, one recovers the solution for incompressible flow which has been the subject of investigation by Spalding, Curle, and others. The present analysis leads to not only the surface heat transfer characteristics but also the details of the temperature field. Moreover, the results are convenient to use.

## 2. PROBLEM STATEMENT AND GOVERNING EQUATION

Figure 1a illustrates the growth of two-dimensional velocity and thermal boundary layer over a smooth object of arbitrary shape situated in an isothermal incoming stream of

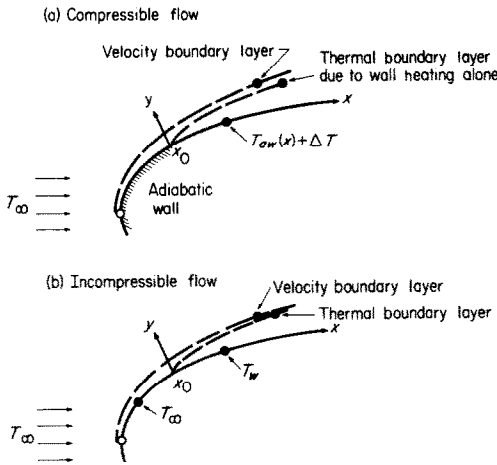


FIG. 1. Physical model and coordinate system.

undisturbed temperature  $T_\infty$ . A front portion of the surface, extending from the forward stagnation to an arbitrary distance  $x_0$ , is adiabatic. For  $x > x_0$ , the wall temperature has a value  $\Delta T$  above the local adiabatic wall temperature  $T_{aw}$ . The flow is laminar and its Reynolds number is sufficiently high that the usual boundary layer simplification is valid. In what follows, we restrict our attention to the situation when the heat is transported as a passive scalar, without affecting the velocity and density distributions in the boundary layer. This is the case studied by Spence and Brown; it requires that the ratio  $\Delta T/T_{aw}$  be much less than unity.\*

The steady state energy boundary layer equation for a viscous, compressible fluid is

$$c_p \rho \left( u \frac{\partial T}{\partial x} + v \frac{\partial T}{\partial y} \right) = u \frac{dp}{dx} + \frac{\partial}{\partial y} \left( k \frac{\partial T}{\partial y} \right) + \mu \left( \frac{\partial u}{\partial y} \right)^2. \quad (4)$$

Since heat is transported as a passive scalar, the full temperature field may be regarded as the sum of two components. The first is that appropriate to the adiabatic wall, which is coupled to the velocity field and satisfies (4). The second is due to the heating over the portion of the wall,

$x > x_0$ , and is the one of our immediate interest. If  $T(x, y)$  is redefined as the temperature field due to the wall heating alone, then

$$c_p \rho \left( u \frac{\partial T}{\partial x} + v \frac{\partial T}{\partial y} \right) = \frac{\partial}{\partial y} \left( k \frac{\partial T}{\partial y} \right), \quad x > x_0 \quad (5)$$

and the appropriate initial and boundary conditions are

$$T(x_0, y) = 0 \quad (6a)$$

$$T(x, 0) = \Delta T, \text{ a constant} \quad (6b)$$

$$T(x, \infty) = 0. \quad (6c)$$

The possibility of decomposing the temperature field into the two components was pointed out in [5].

To facilitate analysis, we introduce a dimensionless temperature function

$$\theta = \frac{T}{\Delta T}, \quad (7)$$

a stream function  $\psi(x, y)$  defined by

$$\rho u = \frac{\partial \psi}{\partial y}, \quad \rho v = -\frac{\partial \psi}{\partial x} \quad (8a, b)$$

and the Howarth variable

$$z = \int_0^y \rho \, dy. \quad (9)$$

With these, (5) becomes

$$\frac{\partial \psi}{\partial z} \frac{\partial \theta}{\partial x} - \frac{\partial \psi}{\partial x} \frac{\partial \theta}{\partial z} = \frac{1}{c_p} \frac{\partial}{\partial z} \left( k \rho \frac{\partial \theta}{\partial z} \right), \quad x > x_0 \quad (10)$$

in the transformed  $(x, z)$  coordinate system.

We now impose the usual restrictions:

$$\left. \begin{aligned} c_p &= \text{constant}, \quad Pr = \text{constant} \\ \text{and} \\ \mu \rho &= \mu_w(x) \rho_w(x), \text{ independent of } y. \end{aligned} \right\} \quad (11)$$

Then, (10) can be rewritten as

$$\frac{\partial \psi}{\partial z} \frac{\partial \theta}{\partial x} - \frac{\partial \psi}{\partial x} \frac{\partial \theta}{\partial z} = \frac{\mu_w \rho_w}{Pr} \frac{\partial^2 \theta}{\partial z^2}, \quad x > x_0. \quad (12)$$

\*  $T_{aw}$  in deg. absolute.

Since

$$\left(\frac{\partial u}{\partial z}\right)_w = \frac{\tau_w}{\mu_w \rho_w} \quad \text{and} \quad \left(\frac{\partial^2 u}{\partial z^2}\right)_w = \frac{1}{\mu_w \rho_w^2} \frac{dp}{dx}, \quad (13a, b)$$

the first two nonvanishing terms in the Taylor expansion for  $u$  are

$$u = \frac{\partial \psi}{\partial z} = \frac{\tau_w}{\mu_w \rho_w} z + \frac{1}{2\mu_w \rho_w^2} \frac{dp}{dx} z^2. \quad (14)$$

It follows that

$$\frac{\partial \psi}{\partial x} = \frac{z^2}{2} \frac{d}{dx} \left( \frac{\tau_w}{\mu_w \rho_w} \right) + \frac{z^3}{6} \frac{d}{dx} \left( \frac{dp}{dx} \frac{1}{\mu_w \rho_w^2} \right). \quad (15)$$

Equation (12) with  $\partial \psi / \partial z$  and  $\partial \psi / \partial x$  respectively defined in (14) and (15) is the governing energy boundary layer equation to be solved in the next section. The associated initial and boundary conditions are

$$\theta(x_0, z) = 0 \quad (16a)$$

$$\theta(x, 0) = 1 \quad (16b)$$

$$\theta(x, \infty) = 0. \quad (16c)$$

For incompressible boundary layer flows of constant properties,  $z = \rho y$  and (12) reduces to

$$u \frac{\partial \theta}{\partial x} + v \frac{\partial \theta}{\partial y} = \frac{\nu}{Pr} \frac{\partial^2 \theta}{\partial y^2}, \quad x > x_0 \quad (17)$$

where

$$\theta = \frac{T - T_\infty}{T_w - T_\infty} \quad (18)$$

$$u = \frac{\tau_w}{\mu} y + \frac{1}{2\mu} \frac{dp}{dx} y^2 \quad (19)$$

and

$$v = -\frac{y^2}{2\mu} \frac{d\tau_w}{dx} - \frac{y^3}{6\mu} \frac{d^2 p}{dx^2}. \quad (20)$$

The corresponding physical model is illustrated in Fig. 1b.

### 3. SOLUTION METHOD AND RESULTS

Since the main objective of the present work

is to improve Lighthill's analysis, we are primarily concerned with the situation when the second term on the right-hand side of (14) or (19) has a subordinate though decisive influence on heat transfer. Therefore, the result is not expected to be applicable to the region close to separation. This, together with the prediction of heat transfer in a boundary layer immediately after reattachment, will be the subject of a separate publication.

#### 3.1 Transformed energy equation

To proceed with the analysis, we consider the following coordinate transformation

$$\begin{matrix} x \\ z \end{matrix} \rightarrow \begin{cases} X = X(x) \\ \xi = zG(x) \end{cases} \quad (21a)$$

$$(21b)$$

where

$$G(x) = \frac{Pr^{\frac{1}{3}}}{3^{\frac{1}{3}}} \left( \frac{\tau_w}{\mu_w \rho_w} \right)^{\frac{1}{3}} \left[ \int_{x_0}^x (\tau_w \mu_w \rho_w)^{\frac{1}{3}} dx \right]^{-\frac{1}{3}} \quad (21c)$$

which tends to infinity as  $x \rightarrow x_0$ . It may be noted that  $\xi$  is the similarity variable of the Lighthill problem, properly generalized to compressible flow under the restrictions prescribed by (11). For the incompressible case, it can be written as

$$\xi = y \frac{Pr^{\frac{1}{3}}}{3^{\frac{1}{3}}} \left( \frac{\rho}{\mu^2} \right)^{\frac{1}{3}} \tau_w^{\frac{1}{3}} \left[ \int_{x_0}^x \tau_w^{\frac{1}{3}} dx \right]^{-\frac{1}{3}} \quad (22)$$

The variable  $X(x)$  is yet to be specified.

Substituting (21) into the energy equation (12), carrying out the indicated differentiation, and making use of the fact that

$$\frac{Pr}{\mu_w \rho_w G} \frac{d}{dx} \left( \frac{\tau_w}{\mu_w \rho_w G^2} \right) = 6 \quad (23)$$

we obtain, after rearranging,

$$\frac{\partial^2 \theta}{\partial \xi^2} + 3\xi^2 \frac{\partial \theta}{\partial \xi} + \frac{Pr}{3\mu_w \rho_w G} \frac{d}{dx} \left[ \left( \frac{\tau_w}{\mu_w \rho_w G^2} \right) \left( \frac{dp/dx}{2\tau_w \rho_w G} \right) \right] \xi^3 \frac{\partial \theta}{\partial \xi}$$

$$= \frac{Pr \tau_w}{(\mu_w \rho_w)^2 G^3} \frac{dX}{dx} \left( 1 + \frac{dp/dx}{2\tau_w \rho_w G} \xi \right) \xi \frac{\partial \theta}{\partial X}. \quad (24)$$

For convenience, we define

$$\varepsilon(x) = \frac{-dp/dx}{2\tau_w \rho_w G} \quad (25)$$

which is dimensionless. It is recognized that  $(\rho_w G)^{-1}$  has the dimension of a length; it is a measure of the local thickness of the thermal boundary layer. The quantity  $\varepsilon(x)$  is physically significant in that it prescribes the relative importance of the influence of pressure gradient on the heat transfer process. When  $\varepsilon(x) = 0$ , the temperature profile becomes similar and corresponds to that of Lighthill. Thus, the present analysis naturally leads to a length scale which arises in formulating the ratio of the pressure gradient term to that due to wall shear in the  $u$ -component velocity representation.

Equation (24) can be simplified by a suitable choice of  $X(x)$ . If we set

$$X = \ln \int_{x_0}^x (\tau_w \mu_w \rho_w)^{\frac{1}{2}} dx, \quad (26)$$

then

$$\frac{dX}{dx} = \frac{(\tau_w \mu_w \rho_w)^{\frac{1}{2}}}{\int_{x_0}^x (\tau_w \mu_w \rho_w)^{\frac{1}{2}} dx} = 9 \frac{(\mu_w \rho_w)^2 G^3}{Pr \tau_w} \quad (27)$$

and (24) simplifies to

$$\begin{aligned} \frac{\partial^2 \theta}{\partial \xi^2} + 3\xi^2 \frac{\partial \theta}{\partial \xi} - \left( 2\varepsilon + 3 \frac{d\varepsilon}{dX} \right) \xi^3 \frac{\partial \theta}{\partial \xi} \\ = 9(1 - \varepsilon\xi) \xi \frac{\partial \theta}{\partial X}. \end{aligned} \quad (28)$$

Since  $G \rightarrow \infty$  as  $x \rightarrow x_0$ , the initial condition (16a) merges with the boundary condition (16c) by the adoption of the  $\xi$ -variable. Accordingly, (28) is to be solved for the following boundary conditions.

$$\theta = 1 \quad \text{for} \quad \xi = 0$$

$$\text{and} \quad \theta = 0 \quad \text{for} \quad \xi \rightarrow \infty. \quad (29a, b)$$

Equation (28), with  $\theta$  defined by (18) and  $\xi$

defined by (22), is directly applicable to the incompressible case.

### 3.2 Series solution and universal functions

With a given  $x_0$  which is arbitrary, both  $\varepsilon$  and  $X$  are known functions of  $x$ . Hence, we may either regard  $\varepsilon$  and  $d\varepsilon/dX$  as functions of  $X$  or, conversely,  $X$  as a function of  $\varepsilon$ . Because of the structure of (28), the latter is the appropriate choice. With this in mind, we write the solution of (28) as follows:

$$\begin{aligned} \theta(X, \xi) = & \theta_0(\xi) + \varepsilon \theta_1(\xi) + \varepsilon^2 \theta_2(\xi) \\ & + \varepsilon^3 \theta_3(\xi) + \dots \\ & + \frac{d\varepsilon}{dX} \phi_1(\xi) + \varepsilon \frac{d\varepsilon}{dX} \phi_2(\xi) + \dots \\ & + \frac{d^2\varepsilon}{dX^2} \psi_1(\xi) + \varepsilon \frac{d^2\varepsilon}{dX^2} \psi_2(\xi) + \dots \\ & + \frac{d^3\varepsilon}{dX^3} \omega_1(\xi) + \varepsilon \frac{d^3\varepsilon}{dX^3} \omega_2(\xi) + \dots \\ & + \frac{d^4\varepsilon}{dX^4} \zeta_1(\xi) + \varepsilon \frac{d^4\varepsilon}{dX^4} \zeta_2(\xi) + \dots \\ & + \dots \end{aligned} \quad (30)$$

with  $\theta_0(0) = 1$ ;

$$\begin{aligned} \theta_1(0) = \theta_2(0) = \dots = \phi_1(0) = \dots \\ = \psi_1(0) = \dots = \omega_1(0) = \dots \\ = \zeta_1(0) \dots = 0 \end{aligned} \quad (31a)$$

and

$$\begin{aligned} \theta_0(\infty) = \theta_1(\infty) = \theta_2(\infty) = \dots = \phi_1(\infty) \\ = \dots = \psi_1(\infty) = \dots, \text{etc.} = 0. \end{aligned} \quad (31b)$$

Upon substituting (30) into (28) and equating coefficients of terms containing  $\varepsilon, \varepsilon^2, \dots, d\varepsilon/dX, \varepsilon(d\varepsilon/dX), \dots, d^2\varepsilon/dX^2$ , etc., we obtain a sequence of second order, linear ordinary differential equations as follows (the primes denote differentiation with respect to  $\xi$ ):

$$\theta_0'' + 3\xi^2 \theta_0' = 0 \quad (32a)$$

$$\theta_1'' + 3\xi^2 \theta_1' = 2\xi^3 \theta_0' \quad (32b)$$

etc. In general, for  $n > 1$ .

$$\theta''_n + 3\xi^2\theta'_n = 2\xi^3\theta'_{n-1} \quad (32c)$$

...

$$\phi''_1 + 3\xi^2\phi'_1 = 3\xi^3\theta'_0 + 9\xi\theta_1 \quad (33a)$$

$$\begin{aligned} \phi''_2 + 3\xi^2\phi'_2 &= 3\xi^3\theta'_1 + 2\xi^3\phi'_1 \\ &\quad - 9\xi^2\theta_1 + 18\xi\theta_2 \end{aligned} \quad (33b)$$

...

$$\psi''_1 + 3\xi^2\psi'_1 = 9\xi\phi_1 \quad (34a)$$

$$\psi''_2 + 3\xi^2\psi'_2 = 2\xi^3\psi'_1 - 9\xi^2\phi_1 + 9\xi\phi_2 \quad (34b)$$

...

$$\omega''_1 + 3\xi^2\omega'_1 = 9\xi\psi_1 \quad (35a)$$

$$\omega''_2 + 3\xi^2\omega'_2 = 2\xi^3\omega'_1 - 9\xi^2\psi_1 + 9\xi\psi_2 \quad (35b)$$

and

$$\zeta''_1 + 3\xi^2\zeta'_1 = 9\xi\omega_1 \quad (36a)$$

$$\zeta''_2 + 3\xi^2\zeta'_2 = 2\xi^3\zeta'_1 - 9\xi^2\omega_1 + 9\xi\omega_2 \quad (36b)$$

etc.

An inspection of the foregoing set of equations (32)–(36), and their boundary conditions (31a, b) shows that all functions are *universal*. As such, they can be tabulated once and for all. This feature makes the determination of local heat transfer and temperature profile in the boundary layer a straightforward procedure.

Equation (32a) with the boundary conditions  $\theta_0(0) = 1$  and  $\theta_0(\infty) = 0$  can be integrated in closed form. The solution is

$$\theta_0 = 1 - \frac{\Gamma(\frac{1}{3}, \xi^3)}{\Gamma(\frac{1}{3})} \quad (37)$$

and

$$\theta'_0(0) = -\frac{3}{\Gamma(\frac{1}{3})} = -1.11985. \quad (38)$$

As it turned out, every equation of the set (32) can be so integrated and expressed in terms of a linear combination of the incomplete gamma functions. For instance,

$$\theta_1 = \frac{\Gamma(\frac{2}{3})}{3\Gamma^2(\frac{1}{3})} \Gamma(\frac{1}{3}, \xi^3) - \frac{1}{2\Gamma(\frac{1}{3})} \Gamma(\frac{5}{3}, \xi^3) \quad (39)$$

and

$$\theta'_1(0) = \frac{\Gamma(\frac{2}{3})}{\Gamma^2(\frac{1}{3})} = 0.18868. \quad (40)$$

However, there is no real need for providing such expressions since the numerical data can be quickly generated on a modern digital computer once the wall derivatives are known. The latter and those of other functions have been evaluated and are listed in Table 1. An abbreviated tabulation of the twelve functions is given in Table 2. It is provided for those who desire the details of the temperature field but do not have access to a computing facility.

The local heat flux at wall is

$$\begin{aligned} q_w &= -k_w \left( \frac{\partial T}{\partial y} \right)_w = \Delta T k_w \rho_w G \left[ -\frac{\partial \theta}{\partial \xi}(X, 0) \right] \\ &= 3^{-\frac{1}{3}} \Delta T Pr^{\frac{1}{3}} \frac{k_w}{\mu_w} (\tau_w \mu_w \rho_w)^{\frac{1}{3}} \\ &\quad \times \left[ \int_{x_0}^x (\tau_w \mu_w \rho_w)^{\frac{1}{3}} dx \right]^{-\frac{1}{3}} \cdot \left[ -\frac{\partial \theta}{\partial \xi}(X, 0) \right] \end{aligned} \quad (41a)$$

where

$$\begin{aligned} \frac{\partial \theta}{\partial \xi}(X, 0) &= \theta'_0(0) + \varepsilon \theta'_1(0) + \varepsilon^2 \theta'_2(0) \\ &\quad + \varepsilon^3 \theta'_3(0) + \dots \\ &\quad + \frac{d\varepsilon}{dX} \phi'_1(0) + \varepsilon \frac{d\varepsilon}{dX} \phi'_2(0) + \dots \\ &\quad + \frac{d^2\varepsilon}{dX^2} \psi'_1(0) + \varepsilon \frac{d^2\varepsilon}{dX^2} \psi'_2(0) + \dots \\ &\quad + \frac{d^3\varepsilon}{dX^3} \omega'_1(0) + \varepsilon \frac{d^3\varepsilon}{dX^3} \omega'_2(0) + \dots \\ &\quad + \frac{d^4\varepsilon}{dX^4} \zeta'_1(0) + \varepsilon \frac{d^4\varepsilon}{dX^4} \zeta'_2(0) + \dots \\ &\quad + \dots \end{aligned} \quad (41b)$$

For the case studied by Lighthill,  $\varepsilon$  is identically zero and

$$\frac{\partial \theta}{\partial \xi}(X, 0) = -\frac{3}{\Gamma(\frac{1}{3})} = -1.11985.$$

Table 1. Wall derivatives of universal functions

$\theta'_0(0)$	$\theta'_1(0)$	$\theta'_2(0)$	$\theta'_3(0)$	$\phi'_1(0)$	$\phi'_2(0)$
-1.11985	0.18868	0.07271	0.05079	0.05751	0.03600
$\psi'_1(0)$	$\psi'_2(0)$	$\omega'_1(0)$	$\omega'_2(0)$	$\zeta'_1(0)$	$\zeta'_2(0)$
-0.09861	-0.09161	0.11358	0.10676	-0.12004	-0.10557

Accordingly,

$$q_w = 0.5384 \Delta T Pr^{\frac{1}{2}} \frac{k_w}{\mu_w} (\tau_w \mu_w \rho_w)^{\frac{1}{2}} \times \left[ \int_{x_0}^x (\tau_w \mu_w \rho_w)^{\frac{1}{2}} dx \right]^{-\frac{1}{2}} \quad (42)$$

which is identical to Liepmann's generalization of Lighthill's result for compressible flow with the exception of the numerical coefficient for which Liepmann indicated a value of 0.524. Liepmann's analysis was based on the integral energy equation and involved certain assumptions concerning the ratios  $\mu\rho/(\mu_w\rho_w)$  and  $q/q_w$ . The minor discrepancy noted above is not

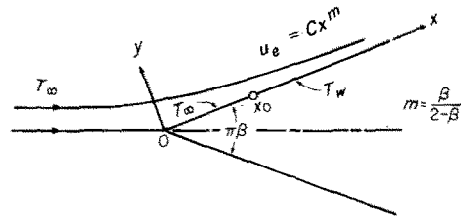


FIG. 2. Forced convection in Falkner-Skan flow.

unexpected. In fact, if  $k$ ,  $\mu$  and  $\rho$  are constants, (42) becomes *exactly* Lighthill's formula.

To develop some feeling on the magnitudes of  $\varepsilon$ ,  $d\varepsilon/dX$ ,  $d^2\varepsilon/dX^2$ , etc., we consider the *incompressible* wedge flow for which the fluid dynamic behaviour is completely describable

Table 2. Universal functions

$\xi$	$\theta_0$	$\theta_1$	$\theta_2$	$\theta_3$	$\phi_1$	$\phi_2$
0.0	1.00000	0	0	0	0	0
0.1	0.88804	0.01886	0.00727	0.00508	0.00576	0.00361
0.2	0.77648	0.03763	0.01452	0.01014	0.01165	0.00734
0.3	0.66630	0.05596	0.02171	0.01515	0.01787	0.01148
0.4	0.55910	0.07319	0.02881	0.02007	0.02452	0.01640
0.5	0.45697	0.08826	0.03578	0.02484	0.03143	0.02246
0.6	0.36224	0.09984	0.04256	0.02944	0.03806	0.02991
0.7	0.27723	0.10653	0.04901	0.03384	0.04355	0.03868
0.8	0.20384	0.10727	0.05479	0.03803	0.04691	0.04822
0.9	0.14326	0.10169	0.05929	0.04197	0.04735	0.05741
1.0	0.09571	0.09041	0.06166	0.04550	0.04455	0.06466
1.1	0.06045	0.07505	0.06103	0.04823	0.03889	0.06824
1.2	0.03589	0.05788	0.05687	0.04954	0.03135	0.06689
1.3	0.01992	0.04125	0.04938	0.04867	0.02322	0.06042
1.4	0.01026	0.02702	0.03956	0.04506	0.01572	0.04993
1.5	0.00489	0.01617	0.02898	0.03873	0.00969	0.03748
1.6	0.00213	0.00880	0.01926	0.03048	0.00541	0.02540
1.7	0.00085	0.00433	0.01153	0.02172	0.00272	0.01545
1.8	0.00031	0.00191	0.00617	0.01386	0.00123	0.00838
1.9	0.00010	0.00076	0.00294	0.00786	0.00049	0.00403
2.0		0.00027	0.00124	0.00393	0.00018	0.00171
2.1			0.00046	0.00172		0.00064
2.2			0.00015	0.00066		0.00021
2.3				0.00022		

Table 2—continued

$\xi$	$\psi_1$	$\psi_2$	$\omega_1$	$\omega_2$	$\zeta_1$	$\zeta_2$
0.0	0	0	0	0	0	0
0.1	-0.00985	-0.00916	0.01135	0.01067	-0.01199	-0.01055
0.2	-0.01961	-0.01825	0.02255	0.02122	-0.02382	-0.02097
0.3	-0.02903	-0.02716	0.03326	0.03140	-0.03509	-0.03097
0.4	-0.03771	-0.03572	0.04288	0.04086	-0.04515	-0.04019
0.5	-0.04511	-0.04375	0.05073	0.04928	-0.05323	-0.04827
0.6	-0.05061	-0.05105	0.05605	0.05632	-0.05853	-0.05489
0.7	-0.05359	-0.05741	0.05825	0.06174	-0.06043	-0.05982
0.8	-0.05363	-0.06249	0.05703	0.06527	-0.05870	-0.06285
0.9	-0.05062	-0.06581	0.05256	0.06661	-0.05358	-0.06371
1.0	-0.04490	-0.06674	0.04546	0.06542	-0.04584	-0.06213
1.1	-0.03725	-0.06466	0.03676	0.06143	-0.03662	-0.05790
1.2	-0.02875	-0.05927	0.02767	0.05469	-0.02721	-0.05112
1.3	-0.02054	-0.05086	0.01929	0.04569	-0.01871	-0.04233
1.4	-0.01349	-0.04043	0.01239	0.03548	-0.01185	-0.03255
1.5	-0.00811	-0.02950	0.00729	0.02535	-0.00687	-0.02302
1.6	-0.00443	-0.01958	0.00391	0.01652	-0.00363	-0.01484
1.7	-0.00219	-0.01173	0.00190	0.00974	-0.00174	-0.00866
1.8	-0.00097	-0.00629	0.00083	0.00515	-0.00075	-0.00453
1.9	-0.00039	-0.00301	0.00032	0.00243	-0.00029	-0.00212
2.0	-0.00014	-0.00127	0.00011	0.00102	-0.00010	-0.00088
2.1		-0.00047		0.00037		-0.00032
2.2		-0.00015		0.00012		-0.00010

by the Falkner-Skan velocity function  $f$  (see e.g. [8]). Referring to Fig. 2, a front portion of the wedge surface, extending over a distance  $x_0$  from the leading edge, is at the temperature  $T_\infty$  of the incoming fluid. The remaining portion,  $x > x_0$ , has a uniform temperature  $T_w$ . Other relevant information is illustrated in the figure. It is well known that, in this case, the velocity at the edge of the boundary layer is

$$u_e = Cx^m \quad (43)$$

where  $C$  is a constant and  $m = \beta/(2 - \beta)$ . If we denote

$$a = f''(0), b = \left(\frac{aPr}{6}\right)^{\frac{1}{2}}, \text{ and } \chi = \left(\frac{x_0}{x}\right)^{\frac{1}{2}(m+1)} \quad (44a, b, c)$$

then

$$\tau_w = a \left(\frac{m+1}{2}\right)^{\frac{1}{2}} (\mu\rho)^{\frac{1}{2}} C^{\frac{1}{2}} x^{(3m-1)/2} \quad (45)$$

$$(\rho G)^{-1} = 2^{\frac{1}{2}} \cdot 3^{\frac{1}{2}} (aPr)^{-\frac{1}{2}} (m+1)^{-\frac{1}{2}} \mu^{\frac{1}{2}} \rho^{-\frac{1}{2}} \times C^{-\frac{1}{2}} x^{(-\frac{1}{2})(m-1)} (1-\chi)^{\frac{1}{2}} \quad (46)$$

$$-\frac{dp}{dx} = \rho C^2 m x^{2m-1} \quad (47)$$

and

$$\varepsilon = \left(-\frac{dp}{dx}\right) (2\tau_w \rho G)^{-1} = \frac{1}{ab} \frac{m}{m+1} (1-\chi)^{\frac{1}{2}} = \frac{\beta}{2ab} (1-\chi)^{\frac{1}{2}} \quad (48)$$

A straightforward calculation shows that

$$\frac{d\varepsilon}{dX} = \frac{d\varepsilon}{dx} \frac{dx}{dX} = \left(\tau_w^{-\frac{1}{2}} \int_{x_0}^x \tau_w^{\frac{1}{2}} dx\right) \frac{d\varepsilon}{dx} = \frac{1}{3} \chi \varepsilon \quad (49a)$$

$$\frac{d^2\varepsilon}{dX^2} = -\frac{1}{3} \chi \left(1 - \frac{4}{3} \chi\right) \varepsilon \quad (49b)$$

$$\frac{d^3\varepsilon}{dX^3} = \frac{1}{3} \chi \left(1 - 4\chi + \frac{28}{9} \chi^2\right) \varepsilon \quad (49c)$$

$$\frac{d^4\varepsilon}{dX^4} = -\frac{1}{3} \chi \left(1 - \frac{28}{3} \chi + \frac{56}{3} \chi^2 - \frac{280}{27} \chi^3\right) \varepsilon, \quad \text{etc.} \quad (49d)$$

Table 3. Extreme values of  $\varepsilon$  in wedge flow,  $\beta/2ab$ 

$\beta$	$m$	$a = f''(0)$	$\beta/2ab$			
			$Pr = 0.1$	$Pr = 1$	$Pr = 10$	$Pr = 100$
-0.19	-0.0867	0.0857	-9.8432	-4.5688	-2.1206	-0.9843
-0.14	-0.0654	0.2397	-1.8401	-0.8541	-0.3964	-0.1840
0	0	0.4696	0	0	0	0
0.2	1/9	0.6867	0.6462	0.2999	0.1392	0.0646
0.5	1/3	0.9277	1.0817	0.5021	0.2331	0.1082
1	1	1.2326	1.4811	0.6875	0.3191	0.1481

For attached boundary layers,  $m > -0.091$ , and, hence,  $0 \leq \chi < 1$ . Accordingly,  $\varepsilon$  ranges between zero and  $\beta/2ab$ ; the numerical values of which for  $Pr$  ranging from 0.1 to 100 are shown in Table 3. The data for  $\beta = -0.19$  are included for reference only since the boundary layer flow is on the verge of separation (theoretical value of  $\beta$  for separation is  $-0.199$ ) which is beyond the intended purpose of the present analysis. It is seen from the table that, except for  $Pr = 0.1$  and for decelerated or highly accelerated flows, the magnitude of the extreme values of  $\varepsilon$  is less than unity. Furthermore, it has been established from (49a)–(49d) that  $0 \leq |(d\varepsilon/dX)/\varepsilon| < 0.333$ ,  $0 \leq |(d^2\varepsilon/dX^2)/\varepsilon| < 0.111$ ,  $0 \leq |(d^3\varepsilon/dX^3)/\varepsilon| < 0.064$ , and  $0 \leq |(d^4\varepsilon/dX^4)/\varepsilon| < 0.055$ . These, together with data given in Tables 1 and 2, suggest that in many practical instances only a limited number of terms in the series (30) and (41b) are needed to provide an accuracy consistent with the two-term approximation of the velocity field.

#### 4. APPLICATION TO SPECIAL CASES—COMPARISON WITH KNOWN RESULTS

##### 4.1 Forced convection in wedge flow due to a step discontinuity in surface temperature

Recently, Chao and Cheema [9] presented a solution for the prediction of heat transfer in Falkner–Skan flow arising from a step discontinuity in the wedge surface temperature. They employed the power series solution for the Falkner–Skan function  $f$  to represent the velocity field. Their expression for the wall heat flux (equations (35) of [9]) was based on the first five nonvanishing terms in the series. When

the Prandtl number is of the order of unity or higher, the higher order terms in the series are not expected to exert any significant influence on the heat transfer process. Hence, their result can be compared with that derived from the present analysis. In making the comparison, we bear in mind that, here, the velocity field is represented by the first two nonvanishing terms and the one which follows is identically zero in incompressible flow.

Upon inserting (45) into (41a) and regarding all properties as constants, we obtain, after some rearrangement,

$$q_w = \left(\frac{a}{6}\right)^{\frac{1}{2}} \frac{k\Delta T}{(2-\beta)^{\frac{1}{2}}} Pr^{\frac{1}{2}} \left(\frac{u_e \rho}{x\mu}\right)^{\frac{1}{2}} (1-\chi)^{-\frac{1}{2}} \times \left[-\frac{\partial \theta}{\partial \xi}(X, 0)\right] \quad (50)$$

where  $\Delta T = T_w - T_\infty$ ,  $u_e = Cx^m$ , and  $\chi = (x_0/x)^{\frac{1}{2}(m+1)}$  as has been defined previously. Since the local skin friction coefficient is

$$\frac{C_f}{2} = \frac{\tau_w}{\rho u_e^2} = \left(\frac{1}{2-\beta} \frac{\mu}{u_e x \rho}\right)^{\frac{1}{2}} a, \quad (51)$$

equation (50) can be rewritten in dimensionless form as

$$\frac{q_w}{c_p \rho u_e \Delta T} = \frac{C_f}{2} Pr^{-\frac{1}{2}} (6a^2)^{-\frac{1}{2}} (1-\chi)^{-\frac{1}{2}} \times \left[-\frac{\partial \theta}{\partial \xi}(X, 0)\right]. \quad (52)$$

The dimensionless wall derivative  $(\partial \theta / \partial \xi)(X, 0)$  remains to be evaluated.

To effect a comparison with equation (35) of [9], the variable used by Chao and Cheema is introduced:

$$X_c = \left[ 1 - \left( \frac{x_0}{x} \right)^{\frac{1}{2}(m+1)} \right]^{\frac{1}{2}} \quad (53a)$$

which is related to  $\lambda$  according to

$$\lambda = 1 - X_c^3. \quad (53b)$$

It follows then from (48) and (49) that

$$\begin{aligned} \varepsilon &= MX_c, \quad \frac{d\varepsilon}{dX} = \frac{1}{3} MX_c(1 - X_c^3), \\ \frac{d^2\varepsilon}{dX^2} &= \frac{1}{9} MX_c(1 - 5X_c^2 + 4X_c^6), \\ \frac{d^3\varepsilon}{dX^3} &= \frac{1}{27} MX_c(1 - 21X_c^3 + 48X_c^6 - 28X_c^9), \\ \frac{d^4\varepsilon}{dX^4} &= \frac{1}{81} MX_c(1 - 85X_c^3 + 420X_c^6 - 616X_c^9 \\ &\quad + 280X_c^{12}), \text{ etc.} \end{aligned} \quad (54)$$

where  $M = \beta/2ab$ . Since  $\varepsilon$  has an unambiguous physical meaning and  $\varepsilon = MX_c$ ,  $X_c$  also has a physical meaning. The fact that the expansion parameter  $X_c$  used in [9] is associated with the relative importance of pressure gradient and wall shear in influencing the convective transport was not recognized earlier. It is also of interest to note that, in the present instance, the derivatives  $d\varepsilon/dX$ ,  $d^2\varepsilon/dX^2$ , etc., are expressible as polynomials of  $X_c$ .

Upon inserting (54) into (41b) and using the data of Table 1, we obtain

$$\begin{aligned} -\frac{\partial\theta}{\partial X}(X, 0) &= 1.1198 - 0.1996 MX_c \\ &\quad - 0.0771 M^2 X_c^2 - 0.0508 M^3 X_c^3 \\ &\quad + \text{terms involving } M^4 X_c^4, M X_c^4, \text{ etc.} \end{aligned} \quad (55)$$

The expression for wall flux presented in [9] is identical to (52) but with the dimensionless wall derivative given by

$$-\frac{\partial\theta}{\partial X}(X, 0) = 1.1198 - 0.2000 MX_c$$

$$\begin{aligned} &- 0.0736 M^2 X_c^2 - 0.0465 M^3 X_c^3 \\ &\quad + 0.0207 \frac{2\beta - 1}{Pr} X_c^3 \\ &\quad + \text{terms involving } M^4 X_c^4, X_c^4, \text{ etc.} \end{aligned} \quad (56)$$

As expected, the first term on the right-hand side of (55) and that of (56) are in exact agreement. It represents the contribution of the linear component of the velocity profile and corresponds to that given by Lighthill [1]. The two second terms are almost identical. The following two corresponding terms exhibit increasing discrepancies; however, they remain tolerable.\* Since the present analysis is primarily concerned with the situation for which  $\varepsilon$  is, at most, of the order unity, the overall agreement between the two expressions is considered satisfactory. Equation (56) contains a term involving  $(2\beta - 1)/Pr$ . It arises from the *third* nonvanishing term in the series expansion for  $u$ ; hence, it is missing in (55). This deficiency is inherent with the two-term representation for  $u$ . When  $\beta = 1$  (stagnation flow),  $Pr = 0.7$  (gases), and  $X_c \sim 1$ , its contribution may become comparable to the two preceding terms in the series. Since it is of the opposite sign, it tends to nullify the effect of the term which immediately precedes it.

The foregoing result demonstrates that the new formula (41) is decisively superior to Lighthill's.

#### 4.2 Local Nusselt number for a circular cylinder of uniform temperature in cross flow

In this second example, we consider the determination of the local heat transfer coefficient over the front portion of a long circular cylinder of diameter  $D$ , transversely located in a uniform incoming flow of undisturbed velocity  $U_\infty$  and temperature  $T_\infty$ . Its surface is held at a uniform temperature  $T_w$ . It is customary to define the local Nusselt number for this case as

$$Nu = \frac{hD}{k} = \frac{q_w D}{k(T_w - T_\infty)}. \quad (57)$$

\* The discrepancies are expected to diminish, if more terms are included in the series (30).

Consequently, (41a) may be rearranged to read (for constant properties and  $x_0 = 0$  appropriate to uniform surface temperature)

$$\frac{Nu}{Re^{\frac{1}{2}} Pr^{\frac{1}{3}}} = \frac{1}{3^{\frac{1}{2}}} \left( \frac{D}{U_{\infty}} \right)^{\frac{1}{2}} \frac{1}{(\mu\rho)^{\frac{1}{2}}} \left( \frac{\tau_w^{\frac{1}{2}}}{\int_0^x \tau_w^{\frac{1}{2}} dx} \right)^{\frac{1}{2}} \cdot \left[ -\frac{\partial\theta}{\partial X}(X, 0) \right] \quad (58)$$

in which  $Re = U_{\infty} D \rho / \mu$ . To proceed with the calculation, we need an expression for  $\tau_w$ . For that purpose, we employ the experimentally measured  $u_e(x)$  which, according to Hiemenz, for air flowing at  $Re = 18500$ , can be well represented by the empirical equation,

$$\frac{u_e}{U_{\infty}} = 3.6314 \left( \frac{x}{D} \right) - 2.1709 \left( \frac{x}{D} \right)^3 - 1.5144 \left( \frac{x}{D} \right)^5 \quad (59)$$

The wall shear can be calculated by the Blasius' procedure; a detailed account of which is given in [8]. The result is

$$\tau_w = 3.0157(\mu\rho)^{\frac{1}{2}} \frac{U_{\infty}^{\frac{1}{2}}}{R^{\frac{1}{2}}} \times \zeta(1 - 0.3513\zeta^2 - 0.06765\zeta^4) \quad (60)$$

where  $R = D/2$  and  $\zeta = x/R$ . Hence,

$$\rho G = \frac{Pr^{\frac{1}{3}}}{3^{\frac{1}{2}}} \left( \frac{\rho}{\mu^2} \right)^{\frac{1}{2}} \tau_w^{\frac{1}{2}} \left( \int_0^x \tau_w^{\frac{1}{2}} dx \right)^{-\frac{1}{2}} = 0.7951 Pr^{\frac{1}{3}} \left( \frac{U_{\infty} \rho}{R \mu} \right)^{\frac{1}{2}} (1 - 0.1506\zeta^2 - 0.0479\zeta^4 - 0.0095\zeta^6 - 0.0031\zeta^8 - \dots)$$

and

$$-\frac{dp}{dx} = \rho u_e \frac{du_e}{dx} = 3.2968 \frac{\rho U_{\infty}^2}{R} \zeta(1 - 0.5978\zeta^2 - 0.0894\zeta^4 + 0.0312\zeta^6 + 0.0034\zeta^8 - \dots).$$

Consequently,

$$\varepsilon = \left( -\frac{dp}{dx} \right) (2\tau_w \rho G)^{-1} = 0.6875 Pr^{-\frac{1}{3}} (1 - 0.0959\zeta^2 - 0.0750\zeta^4 - 0.0300\zeta^6 - 0.0112\zeta^8 - \dots). \quad (61)$$

It follows then

$$\frac{d\varepsilon}{dX} = \left( \tau_w^{-\frac{1}{2}} \int_0^x \tau_w^{\frac{1}{2}} dx \right) \frac{1}{R} \frac{d\varepsilon}{d\zeta} = -0.0879 Pr^{-\frac{1}{3}} \zeta^2 (1 + 1.6636\zeta^2 + 1.1474\zeta^4 + 0.6675\zeta^6 + 0.1423\zeta^8 + \dots) \quad (62)$$

and similar expressions for  $d^2\varepsilon/dX^2$ ,  $d^3\varepsilon/dX^3$  and  $d^4\varepsilon/dX^4$ . When the foregoing results are inserted into (58) and (41b), followed by appropriate rearranging, we arrive at the following expression.

$$\frac{Nu}{Re^{\frac{1}{2}} Pr^{\frac{1}{3}}} = 1.1244(1 - 0.1506\zeta^2 - 0.0479\zeta^4 - 0.0095\zeta^6 - 0.0031\zeta^8 - \dots) \times \left[ -\frac{\partial\theta}{\partial X}(X, 0) \right] \quad (63a)$$

with

$$-\frac{\partial\theta}{\partial X}(X, 0) = 1.1198 - 0.1297 Pr^{-\frac{1}{3}} \times (1 - 0.0857\zeta^2 - 0.0689\zeta^4 - 0.0268\zeta^6 - 0.0089\zeta^8 - \dots) - 0.0344 Pr^{-\frac{1}{3}} (1 - 0.1657\zeta^2 - 0.1122\zeta^4 - 0.0299\zeta^6 - 0.0061\zeta^8 - \dots) + \text{terms involving } Pr^{-1}, Pr^{-\frac{2}{3}}, \text{ etc., and of decreasing significance.} \quad (63b)$$

Equation (63a, b) is valid for arbitrary  $Pr$  which is of the order unity or larger, so long as  $u_e(x)$

could be adequately represented by (59). In (63b), the coefficients of  $\zeta^2$ ,  $\zeta^4$ , etc., are evaluated from various sums of numerical series which consist of positive and negative terms. Since the sequence is not always converging, Euler's transformation has been employed and, in so doing, we have adhered to the rules set forth in Meksyn's book [10].

Schmidt and Wenner [11] measured local heat transfer coefficients around cylinders of 50, 100 and 250 mm dia. in transverse air flow. The hollow brass cylinder was heated and kept at a uniform temperature of 100°C by condensing steam. The free stream temperature of the incoming air was 24°C and the maximum air speed was 33.1 m/s. Thus, the temperature range and flow velocity are such that their data could be directly compared with the theoretical prediction based on the constant property assumption.

Their results for  $Re = 15\,550$  and  $21\,200$  are shown plotted in Fig. 3.\* These were chosen for comparison because the empirical  $u_e$ -distribution used in deriving (63) was for  $Re = 18\,500$ . The solid curve is calculated from (63) for  $Pr = 0.70$ . It is seen that the present analysis somewhat underestimates the data in the region close to the front stagnation and overestimates the data for  $\phi$  greater than 60°. The former is the consequence of the neglect of the higher order terms in the velocity profile which would assume some significance when  $Pr = 0.7$  as has already been pointed out in Section 4.1. In this connection, it is pertinent to note that, at the front stagnation, the theoretically correct value of  $Nu/Re^{1/2}$  is 0.9449 for  $Pr = 0.70$ . The corresponding value calculated from (63) with  $\zeta = 0$  is 0.9286 and the average deduced from Schmidt and Wenner experiments for the two Reynolds numbers cited is 0.971. The reason that the present analysis overestimates the data for large  $\phi$  is not clear. It is probably connected with the

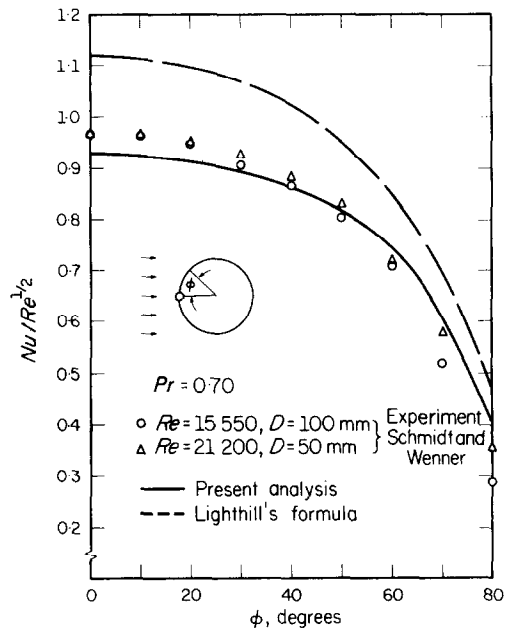


FIG. 3. Comparison between measured and calculated local Nusselt numbers for isothermal cylinders in air flow.

deficiency which still remains of representing the velocity profile by (19). Such deficiency would undoubtedly become less significant in higher Prandtl number fluids. Included in Fig. 3 is the predicted distribution of local Nusselt number according to Lighthill's formula. The improvement offered by the present analysis is obvious.

With the aid of data in Table 2, the temperature profile at different angular locations can be readily calculated from (30). This is illustrated in Fig. 4 for  $\phi = 0$  (front stagnation) and for  $\phi = 57.3$  deg ( $x/R = 1$ ). In order to illustrate the relative thickness of the thermal boundary layer, the abscissa is chosen to be  $(y/R) Re^{1/2}$  instead of  $\zeta$ . They are related according to (22) and, in this case, it becomes

$$\xi = 0.4992 \frac{y}{R} Re^{1/2} (1 - 0.1506\zeta^2 - 0.0479\zeta^4 - 0.0095\zeta^6 - 0.0031\zeta^8 - \dots)$$

since  $Pr = 0.70$ . In general,  $y/R$  varies directly with  $\xi$  and inversely with  $Re^{1/2} Pr^{1/4}$ .

\* Values of  $Nu/Re^{1/2}$  were evaluated from data read from Figs. 4 and 5 of [11].

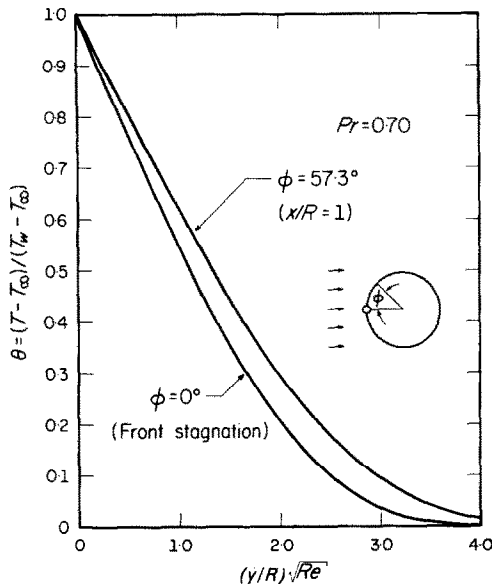


FIG. 4. Temperature distribution at two circumferential locations for isothermal cylinder in air flow.

### 5. CONCLUDING REMARKS

A significant improvement of Lighthill's analysis for heat transfer in boundary layers has been achieved. Equations (30), (41a) and (41b) together with Tables 1 and 2, provide a simple routine procedure for the determination of both the temperature field and local surface heat transfer rates over smooth objects of any arbitrary shape when the wall shear distribution and the streamwise pressure gradient are given. The formulae are directly applicable to surfaces with either a uniform temperature ( $x_0 = 0$ ) or a step discontinuity as described in the text. Objects with any arbitrarily prescribed surface temperature distribution can be handled by the well-known Duhamel's procedure, so long as the diffusion of heat can be considered as a passive scalar. In applying the results, one should bear

in mind the fact that the analysis is based on the two-term representation of the velocity field in the boundary layer and, as such, they remain as approximations to the physical problem.

### 6. ACKNOWLEDGEMENTS

It is a pleasure to acknowledge the assistance of Mr. F. N. Lin who prepared the computer program for the evaluation of the universal functions. Mr. Richard O. Fagbenle helped in calculating the numerical data associated with the second example. Messrs. Lin and Fagbenle are graduate assistants in the department. Thanks are due to Professor A. M. Clausing for his useful suggestions and to the staff of the Mechanical Engineering Publications Office for their skillful preparation of the manuscript. This work is part of a research program on heat transfer in boundary layers partially supported by a National Science Foundation Grant, GK 16270, for which the author is indebted.

### REFERENCES

1. M. J. LIGHTHILL, Contributions to the theory of heat transfer through a laminar boundary layer, *Proc. R. Soc., Lond.* **202A**, 359-377 (1950).
2. H. W. LIEPMANN, A simple derivation of Lighthill's heat transfer formula, *J. Fluid Mech.* **3**, 357-360 (1958).
3. D. B. SPALDING, Heat transfer from surfaces of non-uniform temperature, *J. Fluid Mech.* **4**, 22-32 (1958).
4. N. CURLE, *The Laminar Boundary Layer Equations*, Chapter 6. Clarendon Press, Oxford (1962).
5. D. A. SPENCE and G. L. BROWN, Heat transfer to a quadratic shear profile, *J. Fluid Mech.* **33**, 753-773 (1968).
6. B. J. BELLHOUSE and D. L. SCHULTZ, Determination of mean and dynamic skin friction, separation and transition in low-speed flow with a thin-film heated element, *J. Fluid Mech.* **24**, 379-400 (1966).
7. G. L. BROWN, Theory and application of heated films for skin friction measurement, *Proceedings of the 1967 Heat Transfer and Fluid Mechanics Institute*. Stanford University Press, California (1967).
8. H. SCHLICHTING, *Boundary Layer Theory*, Chapter 9, 6th edn. McGraw-Hill, New York (1968).
9. B. T. CHAO and L. S. CHEEMA, Forced convection in wedge flow with non-isothermal surfaces, *Int. J. Heat Mass Transfer* **14**, 1363-1375 (1971).
10. D. MEKSYN, *New Methods in Laminar Boundary-Layer Theory*, Chapter 7. Pergamon Press, Oxford (1961).
11. E. SCHMIDT and K. WENNER, Wärmeabgabe über den Umfang eines angeblasenen geheizten Zylinders, *Forsch. Geb. Ing.* **12**, 65-73 (1941). English translation: NACA TM 1050 (1943).